Clin Exp Metastasis (2013) 30:165–176
DOI 10.1007/s10585-012-9525-x

RESEARCH PAPER

Trks are novel oncogenes involved in the induction of neovascularization, tumor progression, and nodal metastasis in oral squamous cell carcinoma

Tomonori Sasahira · Nobuhiro Ueda · Kazuhiko Yamamoto · Ujjal K. Bhawal · Miyako Kurihara · Tadaaki Kirita · Hiroki Kuniyasu

Received: 13 February 2012 / Accepted: 30 July 2012 / Published online: 12 August 2012

Abstract The function of tropomyosin receptor kinase (Trk) family including *TrkA*, *TrkB*, and *TrkC* in cancer remains unknown. The role of Trks in oral squamous cell carcinoma (OSCC) was examined. Knockdown of *Trks* provided inhibition of growth or invasion and decrease of apoptosis in OSCC cells, which expressed *Trks* at high levels. *VEGF* expression was associated with *TrkA* and *TrkB* expression; a decrease of *VEGF-C* and *VEGF-D* was observed in OSCC cells with *TrkB* knockdown. *TrkC* did not affect the expression of *VEGF* family. An immunohistochemical analysis of 102 OSCCs showed that *TrkB* expression was related to microvessel density (MVD), lymph vessel density (LVD), and poor prognosis. *TrkC* expression was correlated with clinical stage, lymph node metastasis, MVD, LVD, and poor prognosis. *TrkA* expression was associated with *VEGF* expression, whereas *TrkB expression was associated with the expressions of VEGF*, *VEGF-C* and *VEGF-D*. No significant association was found between the expression of *TrkC* and genes of the *VEGF* family. Expression of *Trks* was not associated with *RUNX3* silencing by methylation in OSCC cells. *Trks* expression was inversely correlated with *RUNX3* expression in the OSCC cases. These results suggested that Trks enhances progression of OSCC through angiogenesis and lymphangiogenesis.

T. Sasahira · U. K. Bhawal · M. Kurihara · H. Kuniyasu (✉)
Department of Molecular Pathology, Nara Medical University School of Medicine, 840 Shijo-cho, Kashihara, Nara 634-8521, Japan
e-mail: cooninh@zb4.so-net.ne.jp

N. Ueda · K. Yamamoto · M. Kurihara · T. Kirita
Department of Oral and Maxillofacial Surgery, Nara Medical University School of Medicine, 840 Shijo-cho, Kashihara, Nara 634-8521, Japan

Keywords Trk · Oral squamous cell carcinoma · Angiogenesis · Lymphangiogenesis · RUNX3

Abbreviation

OSCC	Oral squamous cell carcinoma
Trk	Tropomyosin receptor kinase
NGF	Nerve growth factor
BDNF	Brain derived neurotrophic factor
NT3	Neurotrophin3
RUNX3	Runt-related transcription factor 3
VEGF	Vascular endothelial growth factor
MVD	Microvessel density
LVD	Lymph vessel density
PI3K	Phosphatidylinositol 3′-kinase
BMP	Bone morphogenetic protein
TGF	Transforming growth factor

Introduction

Head and neck cancer constitute the sixth most common malignancy worldwide [1, 2], and the incidence of oral squamous cell carcinoma (OSCC) exceeds 300,000 new cases annually worldwide [3], with a frequency of 3.7 cases per 100,000 people in Japan [4]. OSCC has a high potential for locoregional invasion and nodal metastasis that is characterized by over 50 % patient morbidity and mortality [3, 5]; overall 5-year survival rates have not improved during the past three decades [6].

Tropomyosin receptor kinases (Trks) have a high affinity for neurotrophins, and TrkA, TrkB, and TrkC are the receptors for nerve growth factor (NGF), brain-derived neurotrophic factor (BDNF), and neurotrophin 3 (NT3), respectively [7]. Details about the regulation of Trk expression are unclear, but recently it has been reported

that Trk expression is positively or negatively regulated by runt-related transcription factor 3 (RUNX3) [8, 9], a transcription factor that acts as a tumor suppressor gene. We also observed low or no expression and methylation of *RUNX3* in cases of head and neck cancer [10]. Trks regulate the survival and differentiation of developmental neurons and maintain the growth and action of neuronal synapses throughout adulthood [11]. Trks are also considered oncogenes in many tumors, and several reports have shown that *TrkB* and *TrkC* inhibit apoptosis in cancer cells [12, 13]. Overexpression of *TrkA* was observed in papillary and medullary carcinoma of the thyroid [14, 15] and in ovarian serous carcinoma [14]. Higher levels of TrkB have been found in pancreatic cancer [15], hepatoma [16], prostate cancer [17], ovarian cancer [12], and neuroblastoma [18], and are associated with more aggressive tumor behavior. Chen-Tsai et al. [19] reported that TrkC may predict neural invasion in skin cancer. However, cases with high expression of *TrkA* or *TrkC* have better prognoses in neuroblastoma [20, 21] and TrkC plays a favorable role in medulloblastoma [22]; thus, the detailed role of Trks in cancer is still controversial.

Materials and methods

Cell culture and recombinant human BDNF or NT3 treatment

Human OSCC cell lines, KON, HSC-2, HSC-3, HSC-4, Ca9-22 and SAT, cells were obtained from Health Science Research Resources Bank and maintained in Dulbbeco's modified Eagle's medium (DMEM) (Wako Pure Chemical, Osaka, Japan) supplemented with 10 % fetal bovine serum (FBS) (Sigma Chemical, St. Louis, USA) under the conditions of 5 % CO_2 in air at 37 °C. KON and HSC-3cells have high metastatic potential, HSC-4 cells have low metastatic ability, and HSC-2, Ca9-22, and SAT cells have no ability of metastasis and invasion. Each cell was treated with 10, 20, 30, and 40 μM of Recombinant human NGF (rhNGF) (R&D Systems, Temecula, USA), BDNF (rhBDNF) (R&D Systems), and NT3 (rhNT3) (R&D Systems) treatment were performed.

Quantitative reverse transcription-polymerase chain reaction

Total RNA was extracted using RNeasy Mini Kit (Qiagen, Valencia, USA) and total RNA (1 μg) was synthesized with the ReverTra Ace qRT Kit (Toyobo, Osaka, Japan). Quantitative reverse transcription-polymerase chain reaction (qRT-PCR) were performed on StepOne Plus Real-Time PCR Systems (Applied Biosystems, Foster City, USA) using TaqMan Fast Universal PCR Master Mix (Applied Biosystems) and analyze the relative standard curve quantification method. PCR condition was according to the manufacturer's instructions and ACTB mRNA level was amplified for internal control. TaqMan Gene Expression Assays of TrkA, TrkB, TrkC, VEGF, VEGF-C, VEGF-D, RUNX3, and ACTB were purchased from Applied Biosystems. All PCRs were done at triplicate.

Small interfering RNA

Stealth Select RNAi (siRNA) for TrkA, TrkB, TrkC, and RUNX3 were purchased from Invitrogen (Carlsbad, USA). AllStars Negative Control siRNA was used for control (Qiagen). Twenty-nanometer siRNA were transfected with Lipofectamine 2000 (Invitrogen) according to the provider's recommendations.

Cell growth assay

The cells were seeded at density of 2,000 cells per well of 96-well tissue culture plates and incubated for 48 h at 37 °C. Cell growth was assessed by MTT assay using the incorporation of 3-(4,5-dimethylthiazol-2-yl)-2,5-diphenyltetrazolium bromide (Sigma) [23]. The experiments were performed in triplicate.

In vitro invasion assay

A modified Boyden chamber assay was performed using the BD BioCoat Cell Culture Inserts glued to type IV collagen (Becton–Dickinson, Bedford, USA) as described previously [23]. Cells were suspended in 500 μl of DMEM and placed 4 in the insert. After 48 h incubation at 37 °C, the filters were stained with hematoxylin. The stained cells were counted in whole inserts at 100× magnification. Each experiment was repeated at least three times.

Apoptosis assay

Apoptotic cells were detected by the terminal deoxynucleotidyl transferase (TdT)-mediated dUTP-biotin nick and labeling (TUNEL) assay using the In Situ Cell Death Detection Kit, POD (Roche, Indianapolis, USA). We also confirmed the activation of caspase-3 was detected using CaspACE Assay system, Colorimetric (Promega, Madison, Wisconsin, USA) according to the manufacturer's protocol. The experiments were performed in triplicate.

Immunoblotting

Whole-cell lysate were obtained using M-PER Mammalian Protein Extraction Reagent (Thermo Fisher Scientific Inc.,

Rockford, IL, USA) according to the manufacturer's protocol. Fifty-microgram lysates were subjected to immunoblotting in 12.5 % SDS-PAGE followed by electrotransfer to nitrocellulose filters. The filters were incubated with primary antibody then with peroxidase-conjugated IgG antibody (MBL, Nagoya, Japan). The immune complex was visualized by ECL Western Blotting Detection System (GE Healthcare Ltd., Amersham place, UK). The primary antibodies used were anti-TrkA (Santa Cruz Biotechnology, Santa Cruz, USA, clone C-14), anti-TrkB (Santa Cruz Biotechnology, clone 794), anti-TrkC (Santa Cruz Biotechnology, clone WW6), anti-VEGF-A (Santa Cruz Biotechnology, clone 147), anti-VEGF-C (Santa Cruz Biotechnology, clone F-10), and anti-VEGF-D (Santa Cruz Biotechnology, clone C-18). Anti-GAPDH antibody (Santa Cruz Biotechnology, clone V-18) was used for internal control.

Enzyme-linked immunosorbent assay in culture medium

Cultured medium was filtered with 0.2 μm push filter (Millipore, Bedfold, MA, USA) and enzyme-linked immunosorbent assay (ELISA) system for VEGF (Calbiochem, Darmstadt, Germany), VEGF-C (Bender MedSystems GmbH, San Bruno, CA, USA), VEGF-D (R&D Systems), matrix metalloproteinase (MMP)-2 (R&D Systems), and MMP-9 (R&D Systems) was used. The assay was performed according to the provider's instruction in at least triplicate.

Methylation-specific polymerase chain reaction (MSP)

Genomic DNA was extracted using QIAamp DNA Mini Kit (Qiagen). For the bisulfate modification of DNA, 2 μg of genomic DNA was treated with Epitect Bisulfite Kit (Qiagen) according to the manufacturer's instructions. For analysis of DNA methylation of RUNX3, we carried out MSP using an Epitect MSP Kit (Qiagen). PCR products were separated on 6 % non-denaturing polyacrylamide gels, stained with ethidium bromide (Sigma) and visualized under UV light.

Methylated or unmethylated RUNX3 primer set is as follows [10, 24]: 5′-TTA TGA GGG GTG GTT GTA TGT GGG-3′ and 5′-AAA ACA ACC AAC ACA AAC ACC TCC-3′ for unmethylated RUNX3; 5′-TTA CGA GGG GCG GTC GTA CGC GGG-3′ and 5′-AAA ACG ACC GAC GCG AAC GCC TCC-3′ for methylated RUNX3. All primers were synthesised by Sigma Genosys (Ishikari, Japan).

5-Aza-2′-deoxycytidine treatment

Each cell was seeded at a density of 1×10^6 cells/ml. After 24 h, cells were treated with 1 μM 5-Aza-2′-deoxycytidine (5-Aza-dc) (Sigma) for 4 days. Treat with 300 nm trichostatin A (TSA) (Sigma) was also performed for 24 h. Cells then were harvested for DNA and RNA extractions.

Tissue samples

For immunohistochemical analysis, total of 102 (68 men and 34 woman, Age range, 48–79 years; means, 68.7 years) cases of primary OSCCs containing the deepest lesion and underwent without preoperative therapy were used. Tumor staging was carried out according to TNM classification [25] and the histology of OSCCs are classified according to WHO classification [26]. Medical records and prognostic follow-up data were obtained from the patient database administered by the hospital. For qRT-PCR, 20 OSCCs (13 men and 7 woman, age range, 52–74 years; mean, 63.2 years) and 5 non-tumorous oral mucosa (all samples were gingival mucosa which was excised at the time of the extraction of mandibular third molar, 4 men and 1 woman, age range, 22–40 years; mean, 28.4 years) were used. Samples were frozen immediately in liquid nitrogen and stored at −80 °C until use. All specimens were randomly selected at Nara Medical University Hospital, Kashihara, Japan. Because written informed consent was not obtained, identifying information for all samples was removed before analysis for strict privacy protection; the procedure was in accordance with the Ethical Guidelines for Human Genome/Gene Research enacted by the Japanese Government.

Immunohistochemistry

Consecutive 4 μm sections were cut from each block, and immunohistochemistry was performed as we described previously [27]. Briefly, an immunoperoxidase technique was done following antigen retrieval with microwaving in citrate buffer at 95 °C or pepsin (DAKO, Carpinteria, USA) treatment. After endogenous peroxidase block by 3 % H_2O_2-methanol, anti-TrkA (Santa Cruz Biotechnology, clone C-14), TrkB (Santa Cruz Biotechnology, clone 794), and TrkC (Santa Cruz Biotechnology, clone WW6) antibody, anti-NGF antibody (Santa Cruz Biotechnology, clone H-20), anti-BDNF antibody (R&D Systems, clone UY02), anti-NT3 antibody (CHEMICON, Minneapollis, USA, clone AB1779SP), anti-CD34 antibody (DAKO, clone QBEnd 10), and anti-LYVE-1 antibody (Abcam, Tokyo, Japan, clone ab33682) diluted at 0.5 μg/ml were used for primary antibody and peroxidase-conjugated anti-mouse, anti-rabbit, and anti-goat antibody (MBL) diluted at 0.5 % were used for secondary antibody. According to the attached reference of company, anti-TrkA and TrkC antibody are detection of only each Trks and anti-TrkB antibody is no cross-reaction of TrkB-T1 or TrkBT-Shc and recognizes

only TrkB. The specimens were color-developed with diaminobenzidine (DAB) solution (DAKO) and specimens were counterstained with Meyer's-hematoxylin (Sigma).

Evaluation of immunohistochemistry

Immunoreactivity of Trk, BDNF, and NT3 were classified according to Allred's score (AS) [28] and we divided the immunoreactivity into four grades by AS; Grade 0, AS is 0; Grade 1, AS is 2–4; Grade, AS is 5, 6; Grade 3, AS is 7, 8. Cases with Grade 2 and 3 were regarded as immunopositive [29]. The microvessel density (MVD) and lymphovessel density (LVD) were measured on anti-CD34 and anti-LYVE-1 positive vessels, respectively. Five areas of tissue with the greatest number of distinctly highlighted vessels (the "hot spot") and counted under a 200-fold magnification by microscope and averaged [29–31]. To determine the MVD and LVD, we divided into low or high groups according to density those with values higher the mean value for the entire group and those with than the group mean value [31].

Statistical analysis

Statistical analysis was carried out with JMP8 (SAS Institute, Cary, USA). Statistical differentiation was calculated with unpaired Mann–Whitney *U* test, Student-*t* test, Fischer's exact probability test, and χ^2 test. Disease-free survival was analyzed by the Kaplan–Meier method, and differences between groups were calculated by means of a logrank test. *P* values less than 0.05 were regarded as statistically significant.

Results

Expression and functional analysis of Trks in OSCC cells

At first, six OSCC cells were evaluated for Trk expression by qRT-PCR and immunoblotting. Although TrkA was expressed to a similar extent in each cell, highly metastatic KON and HSC-3 cells exhibited higher expression of TrkB and TrkC than other cells (Fig. 1a).

It was previously reported that Trks regulate angiogenesis [32–34]. Next, we examined the change in VEGF, VEGF-C, and VEGF-D expression levels following Trk siRNA treatment in KON and HSC-3 cells. Gene expression levels of *VEGF*, *VEGF-C*, and *VEGF-D* in KON and HSC-3 cells were higher than in other cells (data not shown). Expression of VEGF was decreased following TrkA or TrkB siRNA treatment, whereas decreases in VEGF-C and VEGF-D expression were observed only with TrkB knockdown in both cell types. No change in the expression of VEGF family was observed following TrkC siRNA treatment. We also observed reduction of secretion levels of VEGF family in TrkA or TrkB siRNA treated OSCC cell culture medium, however, TrkC siRNA did not affect the concentration of VEGF family in culture medium compared to control siRNA treated culture medium (Fig. 1b).

Next, we analyzed the effect of *Trk* on cell growth, invasion, and apoptosis of KON and HSC-3 cells by *Trk* siRNA treatment. Number of the cells, growth ability, and invasive capacity were decreased by *TrkB* and *TrkC* siRNA treatment, respectively (Fig. 1c). Concentration of MMP-2 and MMP-9 in cell culture medium was only decreased by TrkB siRNA treatment (Fig. 1d). Apoptotic cells and caspase-3 activation were increased following *TrkA*, *TrkB*, or *TrkC* siRNA treatment (Fig. 1e).

Recombinant human BDNF and NT3 treatment in KON and HSC-3 cells

We also performed treatments with various concentrations of rhBDNF (a TrkB ligand) and rhNT3 (a TrkC ligand) and examined the effects on cell growth, invasion, and expression of angiogenic/lymphangiogenic factors in KON and HSC-3 cells (Fig. 2a–d). Cells were treated with rhBDNF or rhNT3 and pretreated with 20 nm TrkB or TrkC siRNA, respectively. Both cells showed restoration of growth ability and *VEGF*, *VEGF-C*, and *VEGF-D* expression following treatment with rhBDNF (Fig. 2a, b). Treatment with rhNT3 increased invading cells but did not change the expression levels of the VEGF family in KON and HSC-3 cells (Fig. 2c, d). We also confirmed that rhNGF (ligand of TrkA) treatment and pretreatment with *TrkA* siRNA restored *VEGF* expression dose dependently (Fig. 2e).

Effect of RUNX3 on the expression of Trks in KON and HSC-3 cells

Trk expression is regulated by *RUNX3* in neurons [8, 9]. To confirm whether *RUNX3* regulated *Trk* expression in OSCC, we compared *Trk* expression with the expression and methylation of *RUNX3*. The methylation-specific PCR (MSP) position was located in the *RUNX3* exon1 region [10, 24]. *RUNX3* mRNA was not detected (data not shown) and methylation of *RUNX3* was observed in KON and HSC-3 cells (Fig. 3a). To confirm whether *RUNX3* regulated *Trk* expression in OSCC, we observed the *Trk* expression corresponding to the demethylation of *RUNX3*. Treatment with 5-Aza-dc induced expression of *RUNX3* and significantly decreased *TrkA*, *TrkB*, and *TrkC* expression, whereas treatment with 20 nm *RUNX3* siRNA on day

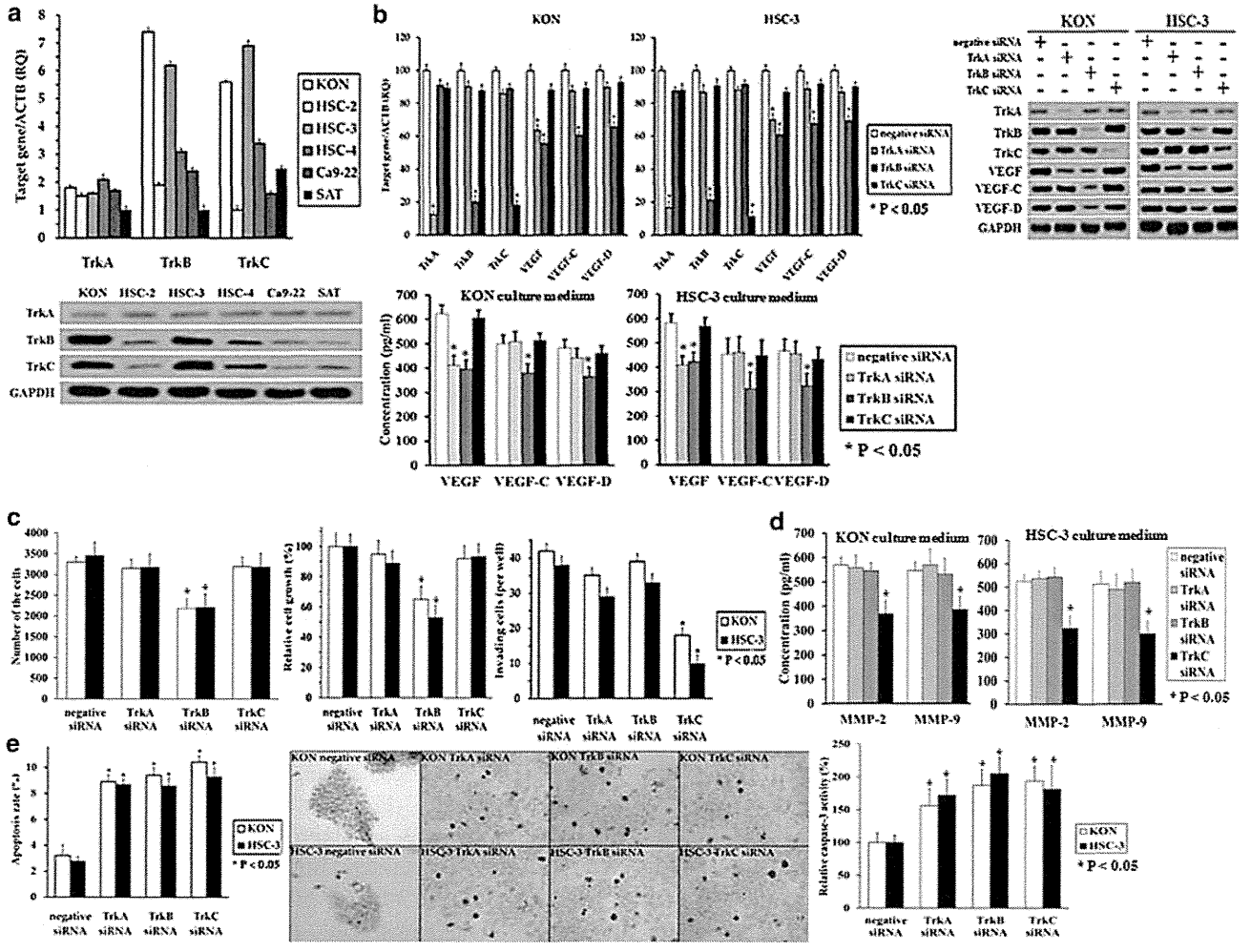

Fig. 1 Effect of Trks in OSCC cell lines. **a** Expression of Trks in six OSCC cells measured using realtime RT-PCR and immunoblotting. Highly metastatic KON and HSC-3 cells showed higher expression of TrkB and TrkC. Expression levels of TrkA was similar extent in each cells. **b–e** Effects of *Trk* siRNA treatment in KON and HSC-3 cells on expression of the *Trk* and VEGF families and secretion of VEGF, VEGF-C, and VEGF-D (**b**), direct cell counting, cell growth, and invasive ability (**c**), secretion of MMP-2 and MMP-9 (**d**), and apoptosis (**e**). Expression of each gene was evaluated by realtime RT-PCR and each protein expression levels was investigated by immunoblotting. Secretion levels of VEGF, VEGF-C, VEGF-D, MMP-2, and MMP-9 were measured by ELISA system. Growth and invasive ability were examined by the MTT assay and an in vitro invasion assay. Apoptotic cells were detected by the TUNEL assay. We also measured caspase-3 activity. Expression and secretion levels of VEGF was decreased by TrkA or TrkB siRNA treatment and decreases in VEGF-C and VEGF-D expression and secretion were observed in TrkB siRNA treated OSCC cells (**b**). Growth ability and invasive capacity were decreased in TrkB and TrkC siRNA treated OSCC cells, respectively (**c**). Decrease of secretion levels of MMP was found in TrkB siRNA treated cells (**d**). Induction of apoptosis and activity of caspase-3 were found in TrkA, TrkB, or TrkC siRNA treated OSCC cells (**e**)

3 after 5-Aza-dc treatment decreased expression levels of *RUNX3*, and restored expression levels of *TrkA*, *TrkB*, and *TrkC* to some extent (Fig. 3b). Treatment with TSA did not change *RUNX3* and *Trk* expression levels (data not shown). These results suggested that *RUNX3* regulated *Trk* expression.

Immunohistochemistry of Trks in cases with OSCC

On the basis of the in vitro results, we examined *Trk* expression in 102 cases with OSCC by using immunohistochemistry. *TrkA*, *TrkB*, and *TrkC* expression levels were negative or very weak in non-tumoral oral mucosa, whereas the immunoreactivity of *TrkA* (Fig. 4a), *TrkB* (Fig. 4b), and *TrkC* (Fig. 4c) was observed in the cell membranes of some OSCC cells. Immunoreactivity of *TrkA*, *TrkB*, and *TrkC* was observed in 90 % (92/102), 31 % (32/102), and 47 % (48/102) of OSCC cases, respectively. Percentages of patients exhibiting co-expression of *TrkA* and *NGF* (Fig. 4d) or *TrkB* and *BDNF* (Fig. 4e) or *TrkC* and *NT3* (Fig. 4f) were 95.7 % (88/92), 88 % (28/32), and 83 % (40/48), respectively. Mean ± SD

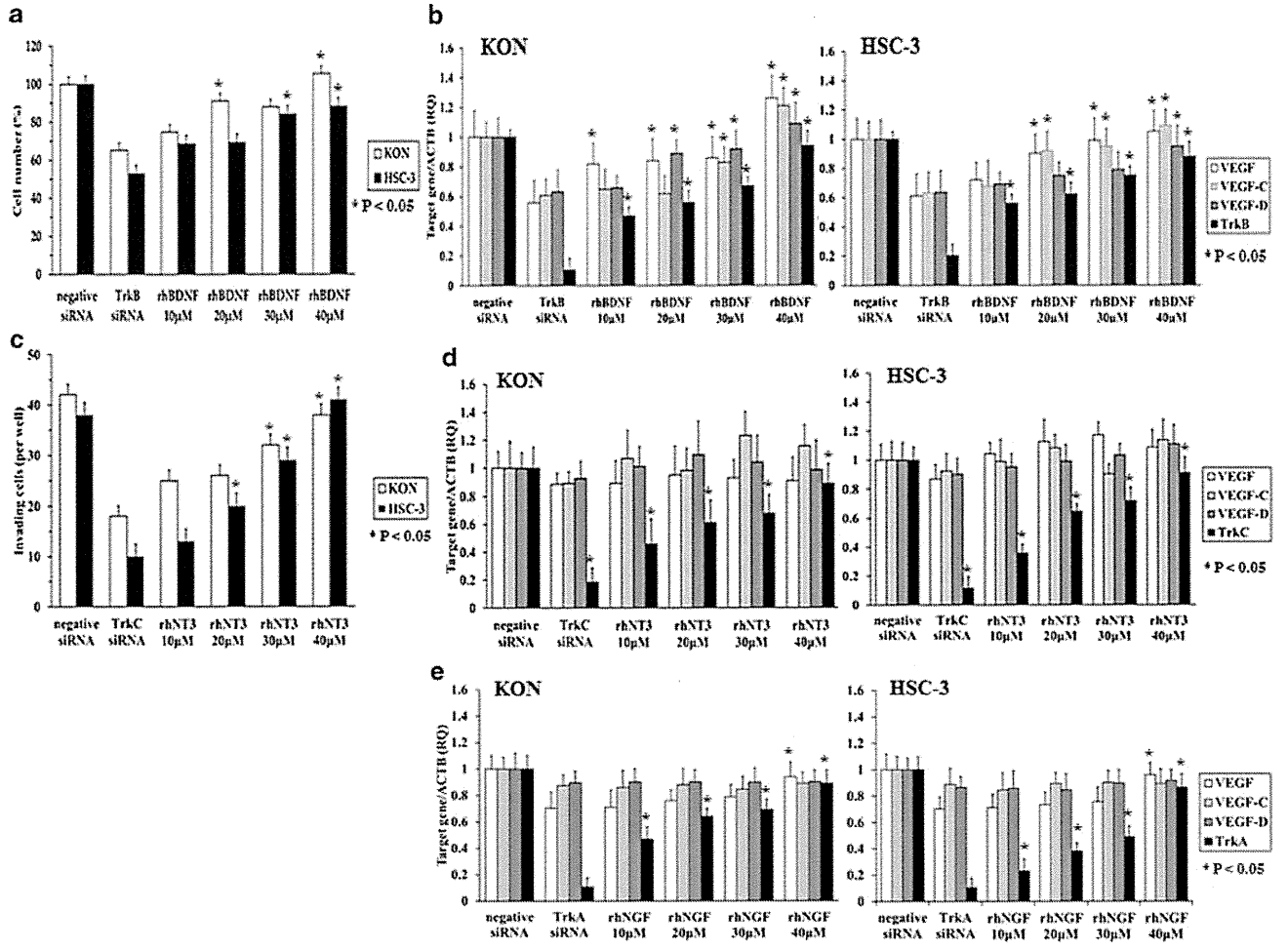

Fig. 2 Effect of BDNF on OSCC cells. Influence of rhBDNF treatment on growth ability (**a**) and *VEGF* family gene expression (**b**), and of rhNT3 treatment on invasive ability (**c**) and expression of genes of the *VEGF* family (**d**). KON and HSC-3 human OSCC cells were used for all experiments. Restoration of growth ability and *VEGF*, *VEGF-C*, and *VEGF-D* expression were found in rhBDNF treated OSCC cells (**a**, **b**). Increase of invading cells was observed but did not change the expression levels of the VEGF family in rhNT3 treated OSCC cells (**c**, **d**)

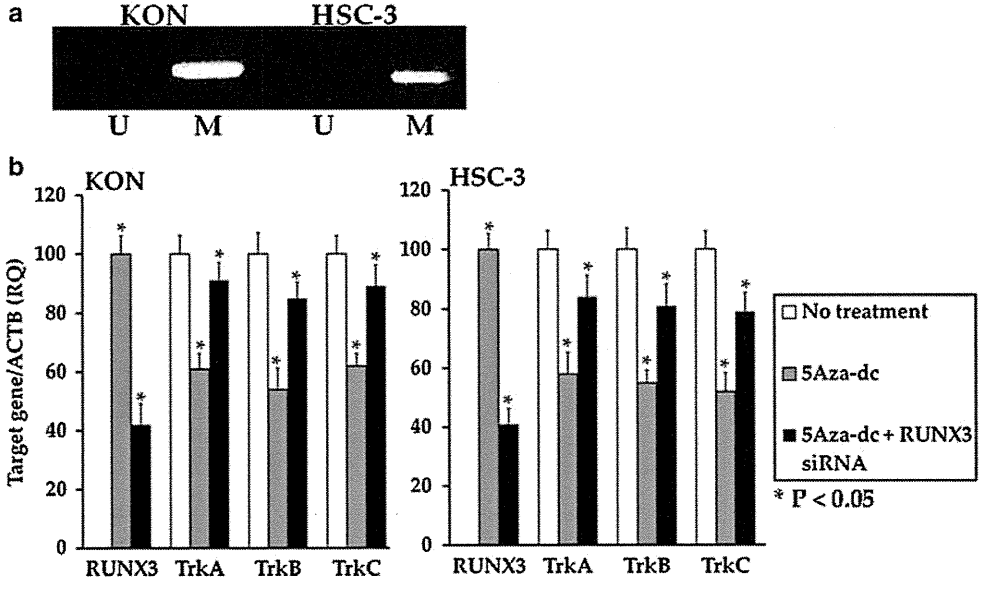

Fig. 3 Methylation status of *RUNX3 gene*. **a** Methylation status of *RUNX3*, evaluated by methylation-specific PCR (MSP) in KON and HSC-3 cells. *U* and *M* means unmethylated and methylated RUNX3, respectively. Methylation of *RUNX3* was observed in KON and HSC-3 cells. **b** Impact of treatment with 5-Aza-dc or 5-Aza-dc + *RUNX3* siRNA on expression of *RUNX3* and Trks in KON and HSC-3 cells. Cells with 5-Aza-dc treatment decreased expression levels of *RUNX3*, and restored expression levels of *TrkA*, *TrkB*, and *TrkC*

(standard deviation) of MVD and LVD in OSCC were 42.41 ± 18.13 and 56.23 ± 23.69, respectively. Cases were divided into a high (Fig. 4g, i) and low group (Fig. 4h, j) based on both parameters. No significant association was found between *TrkA* expression and clinicopathological characteristics; however, a significant relationship was observed between high expression of *TrkB* and MVD ($P = 0.0034$) and LVD ($P = 0.0388$). Immunoreactivity of TrkC was also strongly correlated with gender ($P = 0.0098$), age ($P = 0.0094$), clinical stage ($P = 0.0005$), nodal metastasis ($P = 0.0004$), MVD ($P = 0.0048$), and LVD ($P = 0.0327$) (Table 1).

Disease-free survival analysis

Disease-free survival rates in OSCC patients showed that the prognosis of TrkB-positive cases was significantly worse than that of cases without *TrkB* expression ($P = 0.0166$) (Fig. 5a). High *TrkC* expression cases were also markedly related to a poor prognosis ($P = 0.0036$) (Fig. 5b); however, *TrkA* expression level did not influence survival (data not shown).

Gene expression of Trks, RUNX3, and angiogenic/lymphangiogenic factors in cases with OSCC

Finally, experiments were conducted to confirm the correlation between *Trk* expression and expression of *RUNX3*, *VEGF*, *VEGF-C*, or *VEGF-D*, in 20 cases with OSCC. For controls, five non-tumoral oral epithelium samples were used. In OSCCs, *TrkA*, *TrkB*, and *TrkC* expression was significantly higher than in non-tumorous oral mucosa (Fig. 6). Decreased or absent expression of *RUNX3* was significantly inversely correlated with the overexpression of *TrkA* (Fig. 6a), *TrkB* (Fig. 6b), and *TrkC* (Fig. 6c). We also confirmed that the RUNX3 protein was detected in non-cancerous oral mucosa, whereas it was not detected in OSCC specimens, by immunohistochemistry (data not

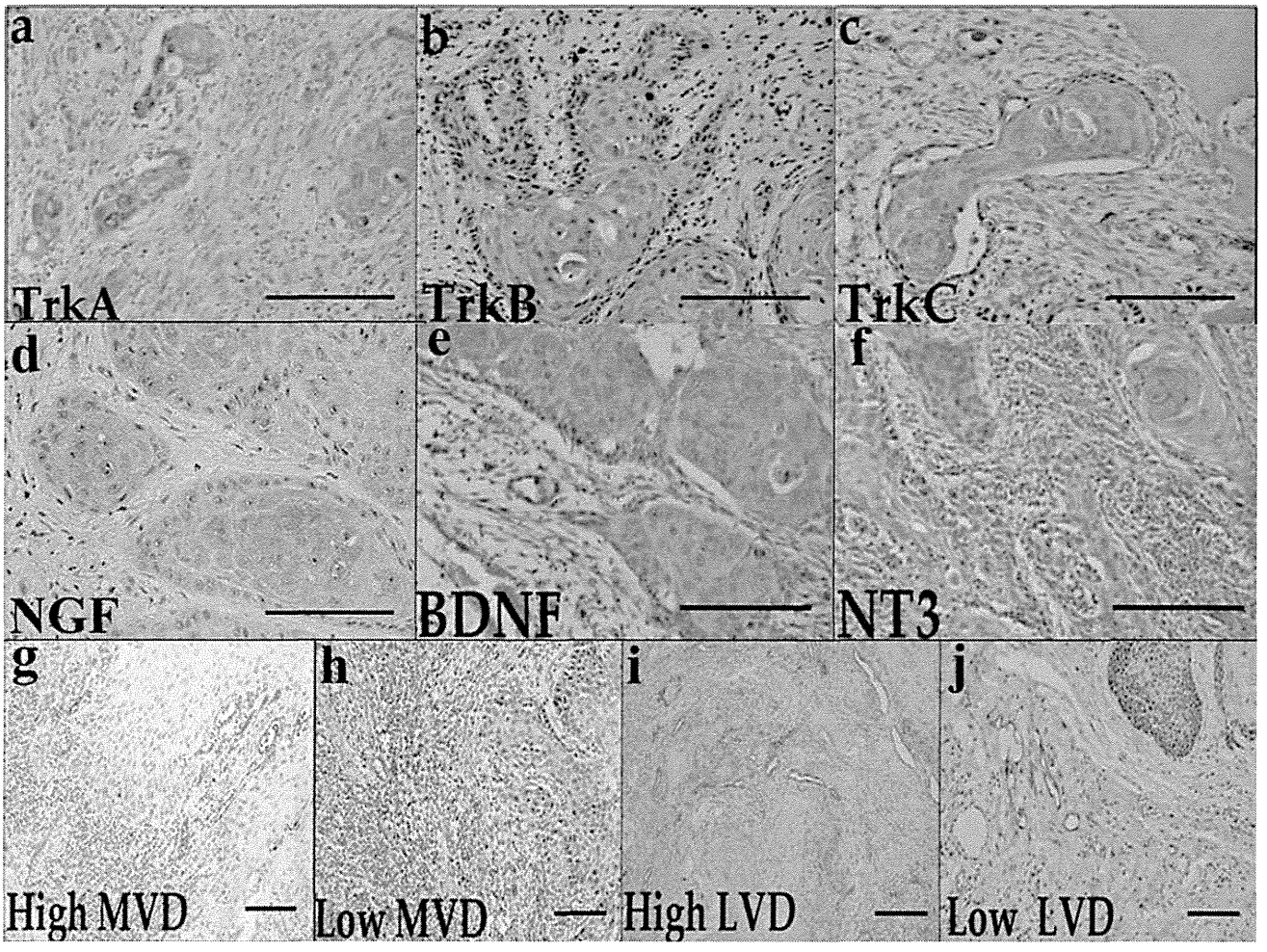

Fig. 4 Expression of Trks in OSCC cases. Immunohistochemical analysis of *TrkA* (**a**), *TrkB* (**b**), *TrkC* (**c**), *NGF* (**d**), *BDNF* (**e**), *NT3* (**f**) expression, MVD (**g**, **h**), and LVD (**i**, **j**). Immunoreactivity of Trks and their ligand were observed in cytoplasm of cancer cells. Original magnification, 400-fold (**a**–**e**) and 200-fold (**g**–**i**). *Bar*, 100 μm

Table 1 Relationship between Trk expression and clinicopathological parameters

Parameters	TrkA		TrkB		TrkC	
	(−)	(+)	(−)	(+)	(−)	(+)
Location						
Tongue	6	41	35	12	25	22
Gingiva	3	31	19	15	17	17
Other	1	20	16	5	12	9
P value	NS		NS		NS	
Gender						
Male	7	61	47	21	30	38
Female	3	31	23	11	24	10
P value	NS		NS		0.0098	
Age						
≤60	1	29	18	12	10	20
>60	9	63	52	20	44	28
P value	NS		NS		0.0094	
Histological differentiation						
Well	9	55	43	21	31	33
Mod, Por	1	37	27	11	23	15
P value	NS		NS		NS	
T classification						
1, 2	7	44	38	13	28	23
3, 4	3	48	32	19	26	25
P value	NS		NS		NS	
Clinical stage						
I, II	5	32	28	9	28	9
III, IV	5	60	42	23	26	39
P value	NS		NS		0.0005	
Nodal metastasis						
Negative	5	50	40	15	38	17
Positive	5	42	30	17	16	31
P value	NS		NS		0.0004	
Microvessel density (MVD)[a]						
Low	4	36	34	6	28	12
High	6	56	36	26	26	36
P value	NS		0.0034		0.0048	
Lymph vessel density (LVD)[a]						
Low	3	44	37	10	30	17
High	7	48	33	22	24	31
P value	NS		0.0338		0.0327	

Relationship between expression of Trk and clinicopathological parameters were calculated by χ^2 test or Fischer's exact t test, respectively. T classification and clinical stage were classified according to the TNM classification

NS not significant; Histological differentiation: *Well* well-differentiated squamous cell carcinoma, *mod* moderately differentiated squamous cell carcinoma, *por* poorly differentiated squamous cell carcinoma

[a] To determine the MVD and LVD, we divided into low or high groups according to density those with values higher the mean value for the entire group and those with than the group mean value

shown). Next, for the gene expression analysis of the Trk and VEGF families, we divided samples into two groups according to expression levels: those with values higher than the mean value for the entire group and those with values lower than the group mean value. The mean ± SD values for each gene were as follows: *TrkA*, 2.71 ± 1.35; *TrkB*, 3.18 ± 2.54; *TrkC*, 3.35 ± 2.65; *VEGF*, 2.59 ± 1.68; *VEGF-C*, 3.94 ± 2.07; and *VEGF-D*, 4.14 ± 2.33. A significant relationship was found between expression levels of *VEGF* and *TrkA* ($P = 0.0349$) or *TrkB* ($P = 0.0124$); *VEGF-C* and *VEGF-D* expression were only correlated with *TrkB* expression ($P = 0.0399$ and $P = 0.0092$, respectively) in cases with OSCC (Table 2). No significant association was found between expression of *TrkC* and *VEGF*, *VEGF-C*, or *VEGF-D*. All the above-mentioned results suggested that Trk participates in angiogenesis and lymphangiogenesis and that Trk expression is regulated by the expression and methylation of *RUNX3*.

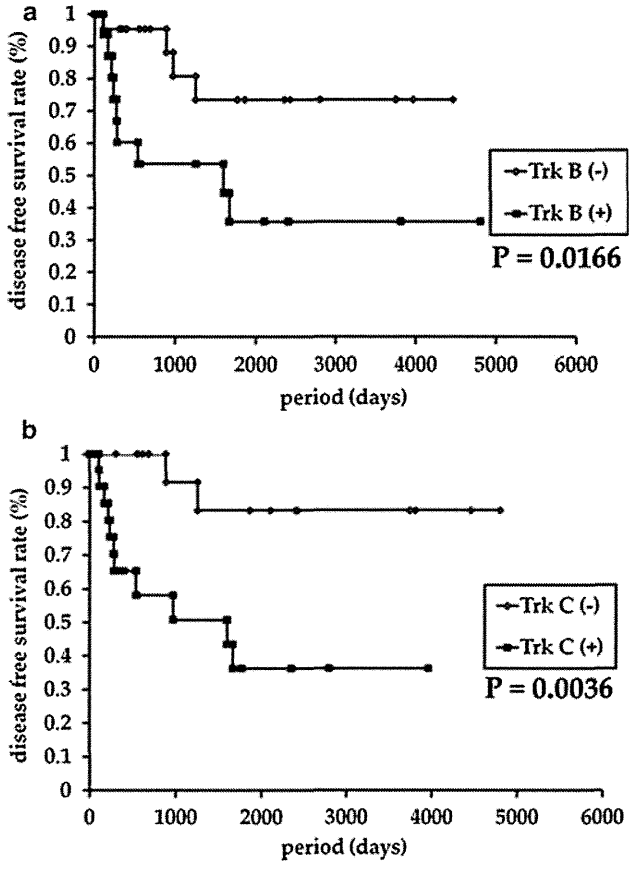

Fig. 5 Relation of expression of Trk B and TrkC and survivals of OSCC cases. Disease-free survival curves for OSCC, using the Kaplan–Meier method. Patients with *TrkB* (**a**) or *TrkC* (**b**) expression had significantly worse outcomes than did patients not showing *TrkB* or *TrkC* expression

Discussion

Trks are considered oncogenes; however, the function of Trks in cancer is still controversial [12–22, 32, 33, 35, 36]. We previously reported that angiogenesis and lymphangiogenesis are significantly associated with tumor progression, nodal metastasis, and poor prognosis in OSCC [31]. We also found that activation of *VEGF* and *VEGF-C* or *VEGF*, *VEGF-C*, and *VEGF-D* promotes angiogenesis or lymphangiogenesis, respectively [31]. Trks are known to accelerate angiogenesis [32–34], whereas the lymphangiogenic roles of Trks are still unknown. In the present study, we examined the expression and function of Trks and compared these to the clinicopathological parameters, including angiogenesis and lymphangiogenesis; expression levels of Trks in OSCC were higher than non-cancerous oral mucosa.

Although *TrkA* expression was correlated with expression and secretion of *VEGF* and the immunopositivity rate of *TrkA* cases with OSCC was very high, no relationship was found between TrkA expression and clinicopathological characteristics by immunohistochemistry. However, induction of apoptosis were observed following TrkA siRNA treatment. It was previously reported that a negative relationship was found between *VEGF* expression and the number of apoptotic cells in cancer [37], and it was also shown that expression levels of *VEGF* were in this step of carcinogenesis [38]. *TrkA* may be involved in oral carcinogenesis by the activation of *VEGF* and reduction of apoptosis.

Several reports indicated that *TrkB* brings about drug resistance by suppression of apoptosis through activation of phosphatidylinositol 3′-kinase (PI3K)-Akt signaling [12, 39] and that tumors expressing high levels of *TrkB* have a bad prognosis [18]. *TrkB* also induces angiogenesis [32]. In OSCC, *TrkB* expression promoted cell growth, inhibited apoptosis, activated *VEGF* expression and secretion, and was significantly associated with angiogenesis and poor prognosis. These findings were mainly in accordance with previous descriptions; no reports are available on the relationship between TrkB expression and lymphangiogenesis via expression of *VEGF*, *VEGF-C*, and *VEGF-D*. Further studies are needed to clarify whether *TrkB* regulates lymphangiogenesis.

It has been shown that *TrkC* is overexpressed in favorable neuroblastoma and medulloblastoma [21, 22], while other reports have shown that *TrkC* act as oncogene in skin cancer [19] and in the inhibition of bone morphogenetic protein (BMP) in breast cancer [35] and of transforming growth factor (TGF)-β signaling in colon cancer [40]. In the present study, we showed that cases with nodal metastasis and worse prognosis exhibited a high expression of *TrkC* as well as a reduction of invasive ability and restoration of apoptotic ability following TrkC siRNA treatment in OSCC. It was surprising that *TrkC* directly promoted angiogenesis and lymphangiogenesis because VEGF family expression and secretion levels were not changed, as shown using the gene knockdown technique for *TrkC*. *TrkC* might be a novel candidate gene, responsible for accelerated angiogenesis and lymphangiogenesis in cancer. We must accurately elucidate the detailed mechanism by which *TrkC* induces angiogenesis/lymphangiogenesis and investigate the possibility that it activates other angiogenic/lymphangiogenic factors in OSCC.

Trks are the receptors for neurotrophins [7] and we observed co-expression of *TrkB* with *BDNF* and *TrkC* with *NT3* in OSCC. We also confirmed the co-expression of *TrkA* with *NGF*. In in vitro analysis, rhBDNF treatment restored cell growth and *VEGF*, *VEGF-C*, and *VEGF-D* expression and rhNT3 treatment increased invasive ability but did not change expression levels of the VEGF family in OSCC cells. We also found that rhNGF treatment restored *VEGF* expression. Although induction of apoptosis and activation of caspase-3 were observed in all Trks

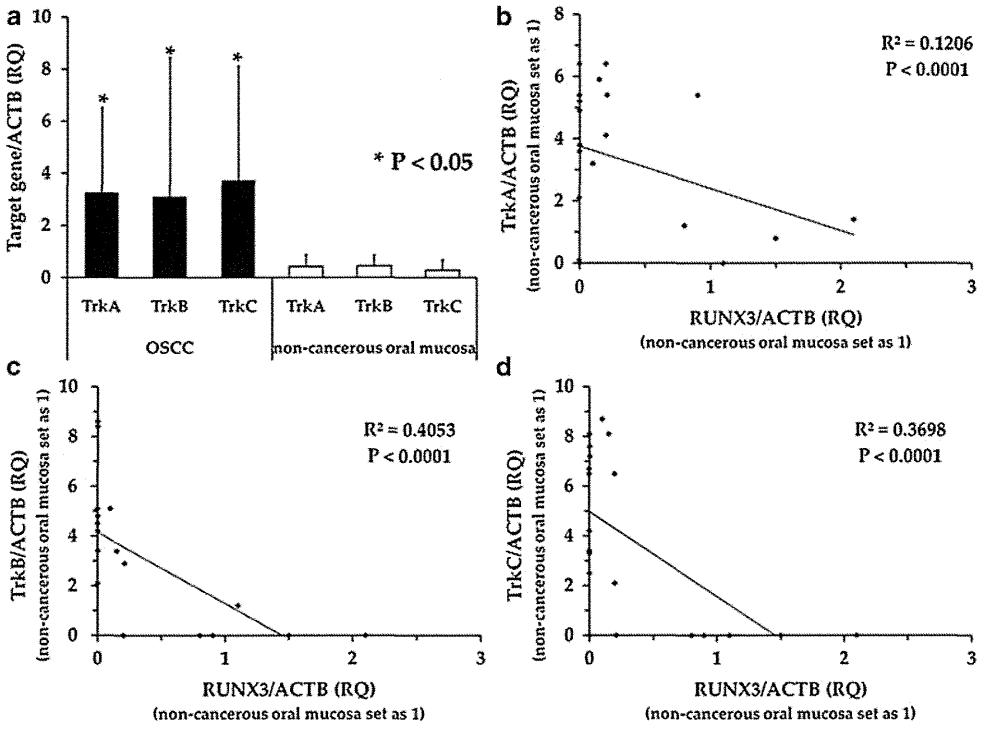

Fig. 6 Expression of *RUNX3* and Trks in OSCC cases. **a** Expression of Trks in non-cancerous oral mucosa and OSCC. Expression levels of Trks in OSCCs were higher than non-cancerous oral mucosa. **b–d** Relationship between expression of *RUNX3* and *TrkA* (**b**), *TrkB* (**c**), or *TrkC* (**d**) in 20 samples of OSCC. Trks expression were reversely associated with expression levels of RUNX3

Table 2 Relationship between gene expression of *Trks* and *VEGF* family

	TrkA		TrkB		TrkC	
	Low	High	Low	High	Low	High
VEGF						
Low	7	2	7	2	6	3
High	3	8	2	9	4	7
P value	0.0349		0.0124		NS	
VEGF-C						
Low	5	3	6	2	7	5
High	5	7	3	9	3	5
P value	NS		0.0399		NS	
VEGF-D						
Low	4	4	8	3	4	4
High	6	6	1	8	6	6
P value	NS		0.0092		NS	

NS not significant

siRNA treated cells, cell growth was only inhibited in *TrkB* siRNA treated cells. Further, inhibition of invasive ability was only found in *TrkC* siRNA treated cells. MMP-2 and MMP-9 makes a basal membrane disintegrate and one of the key factors in the invasion of the cancer cells [29]. In the present study, TrkC displayed regulated MMP-2 and MMP-9 secretion from OSCC cells. These results indicated that *TrkB* or *TrkC* was associated with not only resistance of apoptosis but also cell growth or invasion in cancer cells, respectively. Further studies are in progress to clarify the functional role of Trks in OSCCs.

RUNX3, a transcription factor belonging to the TGF-β superfamily [41], induces apoptosis [42] and is a novel tumor suppressor gene whose expression is decreased or abolished by CpG island hypermethylation of its promoter region in several tumors, including salivary gland cancers [10, 43]. Although it has been reported that *RUNX3* expression was attenuated by *TrkB* expression and that RUNX3 positively regulated expression of *TrkA* and *TrkC* in neuroblastoma and dorsal root ganglion neurons [8, 9], in this study, methylation of *RUNX3* in OSCC revealed a negative association between expression of *RUNX3* and expression of Trks. In this study, we used gingival mucosa, which was removed at the time of the extraction of mandibular wisdom teeth, for the non-cancerous oral mucosa; however, Tsunematsu et al. [44] reported that inflammatory oral epithelium expressed high levels of *RUNX3* compared to the non-inflammatory epithelium. The reason for the discrepancy between our present results and other previous reports may be accounted for by our use of inflammatory oral mucosa for the control.

In conclusion, We clarified TrkB and TrkC are strongly associated with angiogenesis, lymphangiogenesis, tumor progression, nodal metastasis, and poor prognosis and also found that Trks expression are regulated by methylation of *RUNX3* in OSCC. Tumoral vessels are irregular, making it difficult to deliver anti-cancer drugs [31, 45]. Recently, it has been proposed that normalization of tumoral vessels could improve the effectiveness of anti-cancer therapy

[46]. Our present results have suggested that inhibition of Trk signals might be a useful target to normalize of tumoral vessels. An appropriate animal experiment will be needed for further examination of this possibility, and to confirm whether Trks are useful targets for anti-angiogenic and anti-lymphangiogenic therapy in OSCC.

Acknowledgment This work was supported in part by Grant-in-Aid for Scientific Research from Japan Society for the Promotion of Science, Japan.

Conflict of interest We declare that there is not any Financial Support or Relationships which may pose a conflict of interest in the contents of the submitted manuscript.

References

1. Chen YJ, Lin SC, Kao T, Chang CS, Hong PS, Shieh TM, Chang KW (2004) Genome-wide profiling of oral squamous cell carcinoma. J Pathol 204:326–332
2. Hunter KD, Parkinson EK, Harrison PR (2005) Profiling early head and neck cancer. Nat Rev Cancer 5:127–135
3. Lippman SM, Hong WK (2001) Molecular markers of the risk of oral cancer. N Engl J Med 344:1323–1326
4. Tanaka S, Sobue T (2005) Comparison of oral and pharyngeal cancer mortality in five countries: France, Italy, Japan, UK and USA from the WHO Mortality Database (1960–2000). Jpn J Clin Oncol 35:488–491
5. Hershkovich O, Oliva J, Nagler RM (2004) Lethal synergistic effect of cigarette smoke and saliva in an in vitro model: does saliva have a role in the development of oral cancer? Eur J Cancer 40:1760–1767
6. Dos Reis PP, Bharadwaj RR, Machado J, Macmillan C, Pintilie M, Sukhai MA, Perez-Ordonez B, Gullane P, Irish J, Kamel-Reid S (2008) Claudin 1 overexpression increases invasion and is associated with aggressive histological features in oral squamous cell carcinoma. Cancer 113:3169–3180
7. Thiele CJ, Li Z, McKee AE (2009) On Trk: the TrkB signal transduction pathway is an increasingly important target in cancer biology. Clin Cancer Res 15:5962–5967
8. Inoue K, Ito K, Osato M, Lee B, Bae SC, Ito Y (2007) The transcription factor Runx3 represses the neurotrophin receptor TrkB during lineage commitment of dorsal root ganglion neurons. J Biol Chem 282:24175–24184
9. Nakamura S, Senzaki K, Yoshikawa M, Nishimura M, Inoue K, Ito Y, Ozaki S, Shiga T (2008) Dynamic regulation of the expression of neurotrophin receptors by Runx3. Development 135:1703–1711
10. Sasahira T, Kurihara M, Yamamoto K, Bhawal U, Kirita T, Kuniyasu H (2011) Downregulation of runt-related transcription factor 3 (RUNX3) associated with poor prognosis of adenoid cystic and mucoepidermoid carcinomas of the salivary gland. Cancer Sci 102:492–497
11. Tessarollo L (1998) Pleiotropic functions of neurotrophins in development. Cytokine Growth Factor Rev 9:125–137
12. Yu X, Liu L, Cai B, He Y, Wan X (2008) Suppression of anoikis by the neurotrophic receptor TrkB in human ovarian cancer. Cancer Sci 99:543–552
13. Bouzas-Rodriguez J, Cabrera JR, Delloye-Bourgeois C, Ichim G, Delcros JG, Raquin MA, Rousseau R, Combaret V, Bénard J, Tauszig-Delamasure S, Mehlen P (2010) Neurotrophin-3 production promotes human neuroblastoma cell survival by inhibiting TrkC-induced apoptosis. J Clin Invest 120:850–858
14. Davidson B, Reich R, Lazarovici P, Nesland JM, Skrede M, Risberg B, Tropé CG, Flørenes VA (2003) Expression and activation of the nerve growth factor receptor TrkA in serous ovarian carcinoma. Clin Cancer Res 9:2248–2259
15. Sclabas GM, Fujioka S, Schmidt C, Li Z, Frederick WA, Yang W, Yokoi K, Evans DB, Abbruzzese JL, Hess KR, Zhang W, Fidler IJ, Chiao PJ (2005) Overexpression of tropomysin-related kinase B in metastatic human pancreatic cancer cells. Clin Cancer Res 11:440–449
16. Yang ZF, Ho DW, Lam CT, Luk JM, Lum CT, Yu WC, Poon RT, Fan ST (2005) Identification of brain-derived neurotrophic factor as a novel functional protein in hepatocellular carcinoma. Cancer Res 65:219–225
17. Satoh F, Mimata H, Nomura T, Fujita Y, Shin T, Sakamoto S, Hamada Y, Nomura Y (2001) Autocrine expression of neurotrophins and their receptors in prostate cancer. Int J Urol 8:S28–S34
18. Nakagawara A, Azar CG, Scavarda NJ, Brodeur GM (1994) Expression and function of TRK-B and BDNF in human neuroblastomas. Mol Cell Biol 14:759–767
19. Chen-Tsai CP, Colome-Grimmer M, Wagner RF Jr (2004) Correlations among neural cell adhesion molecule, nerve growth factor, and its receptors, TrkA, TrkB, TrkC, and p75, in perineural invasion by basal cell and cutaneous squamous cell carcinomas. Dermatol Surg 30:1009–1016
20. Nakagawara A, Arima-Nakagawara M, Scavarda NJ, Azar CG, Cantor AB, Brodeur GM (1993) Association between high levels of expression of the TRK gene and favorable outcome in human neuroblastoma. N Engl J Med 328:847–854
21. Yamashiro DJ, Nakagawara A, Ikegaki N, Liu XG, Brodeur GM (1996) Expression of TrkC in favorable human neuroblastomas. Oncogene 12:37–41
22. Segal RA, Goumnerova LC, Kwon YK, Stiles CD, Pomeroy SL (1994) Expression of the neurotrophin receptor TrkC is linked to a favorable outcome in medulloblastoma. Proc Natl Acad Sci USA 91:12867–12871
23. Sasahira T, Oue N, Kirita T, Luo Y, Bhawal UK, Fujii K, Yasui W, Kuniyasu H (2008) Reg IV expression is associated with cell growth and prognosis of adenoid cystic carcinoma in the salivary gland. Histopathology 53:667–675
24. Li QL, Ito K, Sakakura C, Fukamachi H, Inoue K, Chi XZ, Lee KY, Nomura S, Lee CW, Han SB, Kim HM, Kim WJ, Yamamoto H, Yamashita N, Yano T, Ikeda T, Itohara S, Inazawa J, Abe T, Hagiwara A, Yamagishi H, Ooe A, Kaneda A, Sugimura T, Ushijima T, Bae SC, Ito Y (2002) Causal relationship between the loss of RUNX3 expression and gastric cancer. Cell 109:113–124
25. Sasaki T, Fujii K, Yoshida K, Shimura H, Sasahira T, Ohmori H, Kuniyasu H (2006) Peritoneal metastasis inhibition by linoleic acid with activation of PPARγ in human gastrointestinal cancer cells. Virchows Arch 448:422–427
26. Sasaki T, Shimura H, Sasahira T, Fujii K, Kuniyasu H (2005) High concentration of deoxycholic acid abrogates in vitro transformation of IEC6 intestinal cells by azoxymethane. J Exp Clin Cancer Res 24:625–631
27. Sasahira T, Akama Y, Fujii K, Kuniyasu H (2005) Expression of receptor for advanced glycation end products and HMGB1/amphoterin in colorectal adenomas. Virchows Arch 446:411–415
28. Allred DC, Harvey JM, Berardo M, Clark GM (1998) Prognostic and predictive factors in breast cancer by immunohistochemical analysis. Mod Pathol 11:155–168
29. Sasahira T, Kirita T, Oue N, Bhawal UK, Yamamoto K, Fujii K, Yasui W, Kuniyasu H (2008) High mobility group box-1-inducible melanoma inhibitory activity is associated with nodal

metastasis and lymphangiogenesis in oral squamous cell carcinoma. Cancer Sci 99:1806–1812
30. Sasahira T, Kirita T, Bhawal UK, Ikeda M, Nagasawa A, Yamamoto K, Kuniyasu H (2007) The expression of receptor for advanced glycation end products is associated with angiogenesis in human oral squamous cell carcinoma. Virchows Arch 450:287–295
31. Sasahira T, Kirita T, Kurihara M, Yamamoto K, Bhawal UK, Bosserhoff AK, Kuniyasu H (2010) MIA-dependent angiogenesis and lymphangiogenesis are closely associated with progression, nodal metastasis and poor prognosis in tongue squamous cell carcinoma. Eur J Cancer 46:2285–2294
32. Nakamura K, Martin KC, Jackson JK, Beppu K, Woo CW, Thiele CJ (2006) Brain-derived neurotrophic factor activation of TrkB induces vascular endothelial growth factor expression via hypoxia-inducible factor-1alpha in neuroblastoma cells. Cancer Res 66:4249–4255
33. Tacconelli A, Farina AR, Cappabianca L, Desantis G, Tessitore A, Vetuschi A, Sferra R, Rucci N, Argenti B, Screpanti I, Gulino A, Mackay AR (2004) TrkA alternative splicing: a regulated tumor-promoting switch in human neuroblastoma. Cancer Cell 6:347–360
34. Cristofaro B, Stone OA, Caporali A, Dawbarn D, Ieronimakis N, Reyes M, Madeddu P, Bates DO, Emanueli C (2010) Neurotrophin-3 is a novel angiogenic factor capable of therapeutic neovascularization in a mouse model of limb ischemia. Arterioscler Thromb Vasc Biol 30:1143–1150
35. Brzezianska E, Pastuszak-Lewandoska D, Lewinski A (2007) Rearrangements of NTRK1 oncogene in papillary thyroid carcinoma. Neuro Endocrinol Lett 28:221–229
36. McGregor LM, McCune BK, Graff JR, McDowell PR, Romans KE, Yancopoulos GD, Ball DW, Baylin SB, Nelkin BD (1999) Roles of trk family neurotrophin receptors in medullary thyroid carcinoma development and progression. Proc Natl Acad Sci USA 96:4540–4545
37. Riedel F, Gotte K, Bergler W, Hormann K (2001) Inverse correlation of apoptotic and angiogenic markers in squamous cell carcinoma of the head and neck. Oncol Rep 8:471–476
38. Larcher F, Robles AI, Duran H, Murillas R, Quintanilla M, Cano A, Conti CJ, Jorcano JL (1996) Up-regulation of vascular endothelial growth factor/vascular permeability factor in mouse skin carcinogenesis correlates with malignant progression state and activated H-ras expression levels. Cancer Res 56:5391–5396
39. Li Z, Jaboin J, Dennis PA, Thiele CJ (2005) Genetic and pharmacologic identification of Akt as a mediator of brain-derived neurotrophic factor/TrkB rescue of neuroblastoma cells from chemotherapy-induced cell death. Cancer Res 65:2070–2075
40. Jin W, Yun C, Kwak MK, Kim TA, Kim SJ (2007) TrkC binds to the type II TGF-beta receptor to suppress TGF-beta signaling. Oncogene 26:7684–7691
41. Hanai J, Chen LF, Kanno T, Ohtani-Fujita N, Kim WY, Guo WH, Imamura T, Ishidou Y, Fukuchi M, Shi MJ, Stavnezer J, Kawabata M, Miyazono K, Ito Y (1999) Interaction and functional cooperation of PEBP2/CBF with Smads. Synergistic induction of the immunoglobulin germline Calpha promoter. J Biol Chem 274:31577–31582
42. Zaidi SK, Sullivan AJ, van Wijnen AJ, Stein JL, Stein GS, Lian JB (2002) Integration of Runx and Smad regulatory signals at transcriptionally active subnuclear sites. Proc Natl Acad Sci USA 99:8048–8053
43. Chuang LS, Ito Y (2010) RUNX3 is multifunctional in carcinogenesis of multiple solid tumors. Oncogene 9:2605–2615
44. Tsunematsu T, Kudo Y, Iizuka S, Ogawa I, Fujita T, Kurihara H, Abiko Y, Takata T (2009) RUNX3 has an oncogenic role in head and neck cancer. PLoS ONE 4:e5892
45. Jain RK, Munn LL, Fukumura D (2002) Dissecting tumour pathophysiology using intravital microscopy. Nat Rev Cancer 2:266–276
46. Jain RK (2005) Normalization of tumor vasculature: an emerging concept in antiangiogenic therapy. Science 307:58–62

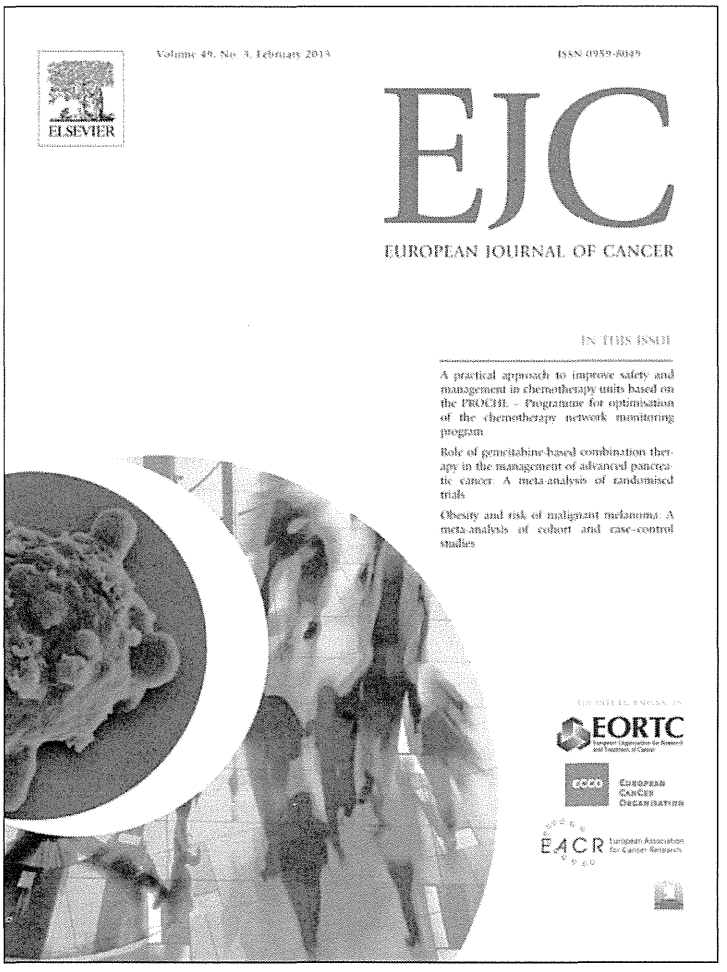

European Journal of Cancer (2013) 49, 741–751

Available at www.sciencedirect.com

SciVerse ScienceDirect

journal homepage: www.ejcancer.info

High mobility group box 1 released from necrotic cells enhances regrowth and metastasis of cancer cells that have survived chemotherapy

Yi Luo [a], Yoshitomo Chihara [a,b], Kiyohide Fujimoto [b], Tomonori Sasahira [a], Masaomi Kuwada [b], Rina Fujiwara [a], Kiyomu Fujii [a], Hitoshi Ohmori [a], Hiroki Kuniyasu [a,*]

[a] *Department of Molecular Pathology, Nara Medical University, Kashihara, Japan*
[b] *Department of Urology, Nara Medical University, Kashihara, Japan*

Available online 3 October 2012

KEYWORDS
HMGB1
Necrosis
Apoptosis
TLR4
RAGE

Abstract The role of the high mobility group box 1 (HMGB1) protein in chemotherapy-induced cell death was examined. CT26 mouse colon cancer cells were treated with trichostatin A (TSA; apoptosis inducer) or doxorubicin (DXR; necrosis inducer). DXR increased HMGB1 concentration in CT26 cell culture medium, whereas TSA did not. In a CT26 bilateral subcutaneous tumour model, DXR or TSA was injected in a single tumour. After injection, serum HMGB1 concentration in DXR-treated mice was 10 times higher than that in TSA-treated mice. After DXR treatment, the contralateral and remnant tumours showed more pronounced growth than did those treated with TSA. In mouse models, lung and liver metastasis was enhanced by DXR but not by TSA. DXR-enhanced metastasis was abrogated by anti-HMGB1 antibody treatment. In a cancer dormancy model, DXR induced regrowth of quiescent CT26 cells. HMGB1 induced tumour necrosis factor-α secretion via Toll-like receptor (TLR)4 in U937 monocytes; however, HMGB1 decreased the number of U937 cells, resulting in restriction of immune activation via receptor for advanced glycation endproducts (RAGE). RAGE showed a more pronounced effect on nuclear factor kappa B activation than did TLR4 in CT26 cells. These findings suggest that HMGB1 released from necrotic cancer cells treated with a necrosis inducer enhances regrowth and metastasis of remnant cancer cells via RAGE activation.

1. Introduction

Cancer chemotherapy aims to reduce the number of cancer cells by induction of cell death. Indeed, necrosis

* *Corresponding author:* Address: Department of Molecular Pathology, Nara Medical University, 840 Shijo-cho, Kashihara, Nara 634-8521, Japan. Tel.: +81 744 22 3051; fax: +81 744 25 7308.
E-mail address: cooninh@zb4.so-net.ne.jp (H. Kuniyasu).

0959-8049/$ - see front matter © 2012 Elsevier Ltd. All rights reserved.
http://dx.doi.org/10.1016/j.ejca.2012.09.016

is a common reaction of cancer cells to anti-cancer drugs. High mobility group box 1 (HMGB1) is a cancer progression-related protein and has been shown to be released from necrotic cells.[1,2] Thus, in view of the massive cell necrosis caused by cancer chemotherapy, the role of HMGB1 in chemotherapy needed to be examined.

The HMGB1 protein is a non-histone chromosomal protein found in eukaryotic cells.[3–5] It is a multifunctional protein that has diverse biological functions in both normal and cancer cells. For instance, HMGB1 possesses DNA-binding properties that permit HMGB1 to regulate multiple processes, including transcription, replication, recombination, DNA repair, genomic stability and activation of Toll-like receptor (TLR)4.[6,7] Furthermore, HMGB1 is associated with cell motility, as observed in neuritis outgrowth,[4] and also with cancer cell invasion.[8] HMGB1 is secreted from activated monocytes, macrophages and natural killer cells, and acts extracellularly as a proinflammatory cytokine.[9,10] Cancer cells also secrete and overexpress HMGB1 by stimulation of growth factors, cytokines and cellular stresses that involve advanced glycation endproducts (AGE) and deoxycholic acid.[11–14] Secreted HMGB1 acts as a ligand to activate the receptor for advanced glycation endproducts (RAGE), thereby inducing cell growth, motility, invasion, angiogenesis and metastasis.[8,12,15–18]

HMGB1 is released from cells by both active and passive processes. Active secretion of HMGB1 is associated with detachment from loosened chromosomes by histone acetylation, HMGB1 hyperacetylation and monomethylation of HMGB1 at Lys42.[14,19,20] The mechanism of cytoplasmic HMGB1 secretion from human monocytes is associated with an atypical endolysosomal-like secretory pathway.[21] In contrast, HMGB1 is released from necrotic cells by passive diffusion.[2] However, HMGB1 is not released from the tightly-packed nuclei of apoptotic cells and triggers inflammation.

HMGB1 is an agonist of RAGE and TLR4; however, both receptors are expressed on cancer cells and immune cells.[22,23] In the present study, we compared the effects of HMGB1 on cancer cell regrowth and metastasis after treatment with necrotic anti-cancer drugs or apoptosis-inducers.

2. Materials and methods

2.1. Cell culture and reagents

CT26 mouse colon cancer cell line was kindly provided from Professor Isaiah J. Fidler (M.D. Anderson Cancer Center, USA).[24] LL2 murine lung cancer cell line and HT29 human colon cancer cell line were purchased (Dainihon Pharmaceutical, Tokyo, Japan). Cells were maintained in Dulbecco's modified essential medium (Sigma Chemical Co., St. Louis, USA) containing 10% foetal bovine serum (Sigma) under the conditions of 5% CO_2 in air at 37 °C. Sodium nitroprusside (SNP; Sigma), trichostatin A (TSA; Wako Pure Chemical, Osaka, Japan), linoleic acid (LA; Sigma), doxorubicin (DXR; Sigma), ethyl pyruvate (EP; Wako), human recombinant HMGB1 and anti-HMGB1 antibody (R&D Systems, Minneapolis, USA) were purchased.

2.2. Assessment of cell growth and apoptosis

Cells growth was assessed by MTT assay according to the previous description.[23] Apoptosis and necrosis were assessed by apoptosis/necrosis detection kit (Enzo Life Sciences, Plymouth Meeting, USA). In the kit, apoptotic and necrotic cells were labelled fluorescently by annexin V-EnzoGold and 7-AAD, respectively. Cells (2000) were observed to determine apoptosis or necrosis under fluorescent microscope. The experiments were performed in triplicate. Lactate dehydrogenase C (LDH) and Terminal deoxynucleotidyl transferase (TdT)-mediated dUTP-biotin nick end labelling (TUNEL) were also examined. Colony formation assay in soft agar gel was performed according to our previous report.[25]

2.3. Cultured medium

CT26 cells (1×10^8) were cultured with regular medium containing 50% inhibitory concentration (IC50) concentration of DXR (0.5 μg/ml) and TSA (62 μg/ml), or PBS for the control for 24 h. The cultured media were collected and filtrated with 0.2 μm filter (Becton-Dickinson Labware, Bedford, USA). CT26 cells were treated with the mixture of fresh regular medium and the cultured medium for 24 h and the living cell number was counted by Autocytometer (Sysmecs, Kobe, Japan).

2.4. Animal model

BALB/c, C57BL6 and athymic nu nu BALB/c mice (male, 4 weeks old), purchased from Japan SLC (Shizuoka, Japan), were maintained according to the institutional guidelines approved by the Committee for Animal Experimentation of Nara Medical University. Single-cell suspensions of CT26 cells (1×10^7) in Hanks solution were injected into the scapular regions of mice at day 1. In the bilateral tumour model, CT26 cells (1×10^7) were injected into the bilateral scapular regions of mice. For a rapid growth model, cell (1×10^8) were inoculated. For metastasis model, CT26 cells (1×10^6) were injected into the spleen and the tail vein to form metastasis in the liver and lung, respectively, at day 6. DXR or TSA were injected into the back tumour at day 8. Serum HMGB1 was examined ay day 9. Anti-HMGB1 antibody (R&D, 5 and 20 μg in 200 μl PBS for 10^7 and 10^8 cells inoculated, respectively) was administrated intraperitoneally at defined date. The dosage

was calculated for neutralising 2 or 8 μg/ml of HMGB1 in a 20-g weight mouse.[26] EP (30 mg/kg body weight) was administrated intraperitoneally. The tumour volume was calculated by a formula of (short diameter/2)^2 × long diameter × π.

2.5. Dormancy model

CT26 cells were treated with LA (200 μg/ml) for 6 weeks, which induced quiescence to the cells. The quiescent CT26 cells (1×10^6) were inoculated in the contralateral side of the back at day 6.[13]

2.6. TUNEL assay

TUNEL assay using the *In Situ* Cell Death Detection Kit, POD (Roche Diagnostics, Indianapolis, USA). The percent frequency of TUNEL-positive cells was calculated from the ratio of positive nuclei to 500 examined nuclei.

2.7. Enzyme-linked immunosorbent assay (ELISA)

Mouse blood was collected from the heart or caudal vein. The blood was rapidly centrifuged by 500*g*, 4 min at 4 °C. The supernatant was used as serum. Cultured medium (200 μl) filtrated with 0.2 μm filter (Becton-Dickinson) was used for ELISA. HMGB1, LDH and TNF-α in serum or cultured medium were measured by each specific ELISA kit (Shinotest, Tokyo, Japan, Uscn Life Science, Uhan, China, and Abnova, Taipei City, Taiwan, respectively). ELISA was performed according to provider's instructions. The experiment was repeated three times.

2.8. Small interfering RNA (siRNA)

Stealth Select RNAi for RAGE, and TLR4 were purchased from Invitrogen (Carlsbad, USA). AllStars siRNA was used for control (Qiagen). siRNA (20 nM) was transfected with Lipofectamine 2000 (Invitrogen) according to the provider's instructions.

2.9. Quantitative reverse transcription-polymerase chain reaction (RT-PCR)

Total RNA was extracted using RNeasy Mini Kit (Qiagen) and total RNA (1 μg) was synthesised with the ReverTra Ace qRT Kit (Toyobo, Osaka, Japan). Quantitative reverse transcription-polymerase chain reaction was performed on StepOne Plus Real-Time PCR Systems (Applied Biosystems, Foster City, USA) using TaqMan Fast Universal PCR Master Mix (Applied Biosystems) and analyse the relative standard curve quantification method. PCR condition was according to the manufacturer's instructions and ACTB mRNA level was amplified for internal control. TaqMan Gene Expression Assays of RAGE, TLR4 and ACTB were purchased from Applied Biosystems. All PCRs were done at triplicate.

2.10. Immunoblot analysis

Whole-cell lysates were prepared as described previously.[23] Nuclear fraction was extracted as described previously.[14] Fifty-microgram lysates were subjected to immunoblot analysis in 12.5% sodium dodecyl sulphate–polyacrylamide gels followed by electrotransfer (SDS–PAGE) to nitrocellulose filters. For examining oxidised HMGB1, the lysates were separated in a non-reduced condition by SDS–PAGE.[26] The immune complex was visualised with an ECL system (Amersham, Aylesbury, UK). Antibodies to nuclear factor kappa B (NFκB) p65, IκB, extracellular signal-regulated protein kinase (ERK)1/2, and phosphorylated ERK1/2 (Santa-Cruz Biotechnology, Santa Cruz, USA), HMGB1 (R&D Systems), and microtubule-associated protein light chain (LC)3 (CosmoBio, Tokyo, Japan) were used for primary reaction.

2.11. Statistical analysis

Statistical analyses of experimental data were performed using Mann–Whitney *U* test, Kruskal–Wallis test with Dunn's multiple comparison test (non-parametric ANOVA). Statistical significance was defined as a two-sided *P* value of less than 0.05.

3. Results

3.1. Effect of cell death inducers on CT26 cell growth

First, we examined the effect of four cell death inducers, SNP, TSA, LA and DXR, on the growth of CT26 mouse colon cancer cells (Fig. 1). Treatment with cell death inducers resulted in a dose-dependent decrease in CT26 cell numbers (Fig. 1a–d). A longer treatment showed that the apoptosis-inducers continued to induce cell decrease, whereas the effect of the necrosis-inducers was close to a plateau (Fig. 1e). A colony formation assay showed that the necrosis-inducers increased the colony number at week 4 in comparison with those at week 2 (Fig. 1f). The induction of apoptosis or necrosis was quantified at the IC50 of cell death inducers (Fig. 1g). LA and DXR induced mainly necrosis, whereas SNP and TSA induced mainly apoptosis. The induction of necrosis and apoptosis were confirmed by LDH release and TUNEL, respectively (Fig. 1h).

3.2. Secondary effect of cell death on remnant cells

To examine the effect of induction of cell death on remnant living cells, we cultured CT26 cells in a medium supplemented with DXR and TSA of the concentrations at

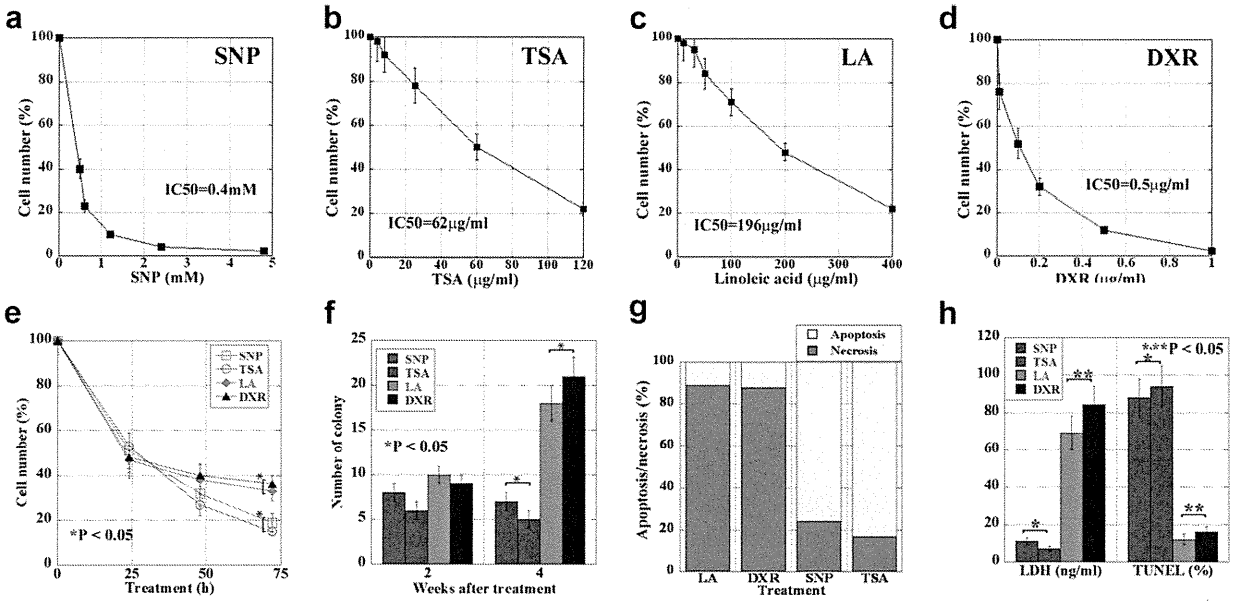

Fig. 1. Effect of cell death inducers on CT26 cell growth. (a–d) The growth inhibitory effect of sodium nitroprusside (SNP), trichostatin A (TSA), linoleic acid (LA) and doxorubicin (DXR) on CT26 cells was examined at various concentrations. Cell number was counted by an autocytometer. The 50% inhibitory concentration (IC50) after 24-h treatment is also indicated. (e) The time course of the cell number treated with SNP, TSA, LA and DXR at the IC50. (f) The colony forming assay after 48-h treatment of SNP, TSA, LA and DXR at the IC50. The colony numbers were counted at 2 and 3 weeks after treatment. (g) The apoptosis/necrosis ratio of dead cells was examined in CT26 cells treated with IC50 for 24 h. (h) To confirm the pro-apoptotic or pro-necrotic effects of SNP, TSA, LA and DXR, LDH concentration in the culture media and Terminal deoxynucleotidyl transferase (TdT)-mediated dUTP-biotin nick end labelling (TUNEL)-positive cell percentage were examined in cells after 48-h treatment of the four agents. Error bars represent standard deviation (SD).

IC50 (Fig. 2a and b) and the half concentration of IC50 (Fig. 2c and d). CT26 cells treated with the medium in which DXR-treated cells were cultured showed growth enhancement in comparison with cells cultured in the control (PBS-treated) medium. In contrast, cells treated with the medium in which TSA-treated cells were cultured did not show growth enhancement. Treatment with DXR of the half concentration of IC50 showed less pronounced effect than that of IC50 DXR treatment ($P < 0.05$). These findings suggest that a specific humoral factor was responsible for the necrotic cell-associated cell growth. Because HMGB1 is a known necrosis sensor, the presence of HMGB1 was examined in the culture medium (CM) of CT26 cells treated with cell death inducers (Fig. 2e). Necrosis inducers (DXR and LA) yielded higher levels of HMGB1 in the CM in a dose-dependent manner in comparison with apoptosis inducers did (TSA and SNP) ($P < 0.0001$). Using the CM of 72-h treatment, CT26 cells treated with 50% DXR-CM and 70% DXR-CM showed $126 \pm 18\%$ and $122 \pm 15\%$ cell numbers, respectively. Oxidised HMGB1 lacks ligand activity.[26,27] The less proliferative effect of 72-h treated DXR-CM than that of 24-h treated DXR-CM might be resulted from increased oxidised HMGB1 portion (Fig. 2f). HMGB1 is reported to enhance cell survival by autophagy induction.[27,28] To examine the pro-autophagy effect of HMGB1, production of LC3 was detected by immunoblotting, which is one of autophagy machinery proteins. In Fig. 2g, necrosis-inducers increased LC3 levels; however, apoptosis-inducers did not.

3.3. Effect of cell death inducers on HMGB1 release in a mouse tumour model

CT26 subcutaneous tumours on the back of BALB/c mice were treated with DXR (5 and 10 μg/mouse) or TSA (0.6 and 1.2 mg/mouse) by intraperitoneal (i.p.) administration. DXR treatment produced necrotic areas; however, a few apoptotic cells were also observed in the tumour (Fig. 3a). In contrast, TSA treatment resulted in numerous TUNEL-positive apoptotic cells, but failed to produce necrotic areas. TSA treatment showed that the number of apoptotic cells was increased in a dose-dependent manner and was higher than that by DXR treatment (Fig. 3b, $P < 0.0001$). In contrast, DXR treatment showed that serum LDH was increased in a dose-dependent manner and was higher than that by TSA treatment (Fig. 3c, $P < 0.0001$). Furthermore, in the DXR-treated mice, the serum concentration of HMGB1 was increased in a dose-dependent manner and was higher than that in the TSA-treated mice (Fig. 3d). The regrowth after the injection of DXR of the tumours showed more pronounced than that in TSA-treated tumours (Fig. 3e).

3.4. Effect of cell death on growth of remnant tumours

The necrosis inducer DXR was shown to enhance cell growth of remnant cancer cells *in vitro*. Thus, to examine the situation *in vivo*, we used a bilateral subcutaneous mouse tumour model. Regrowth of an injected

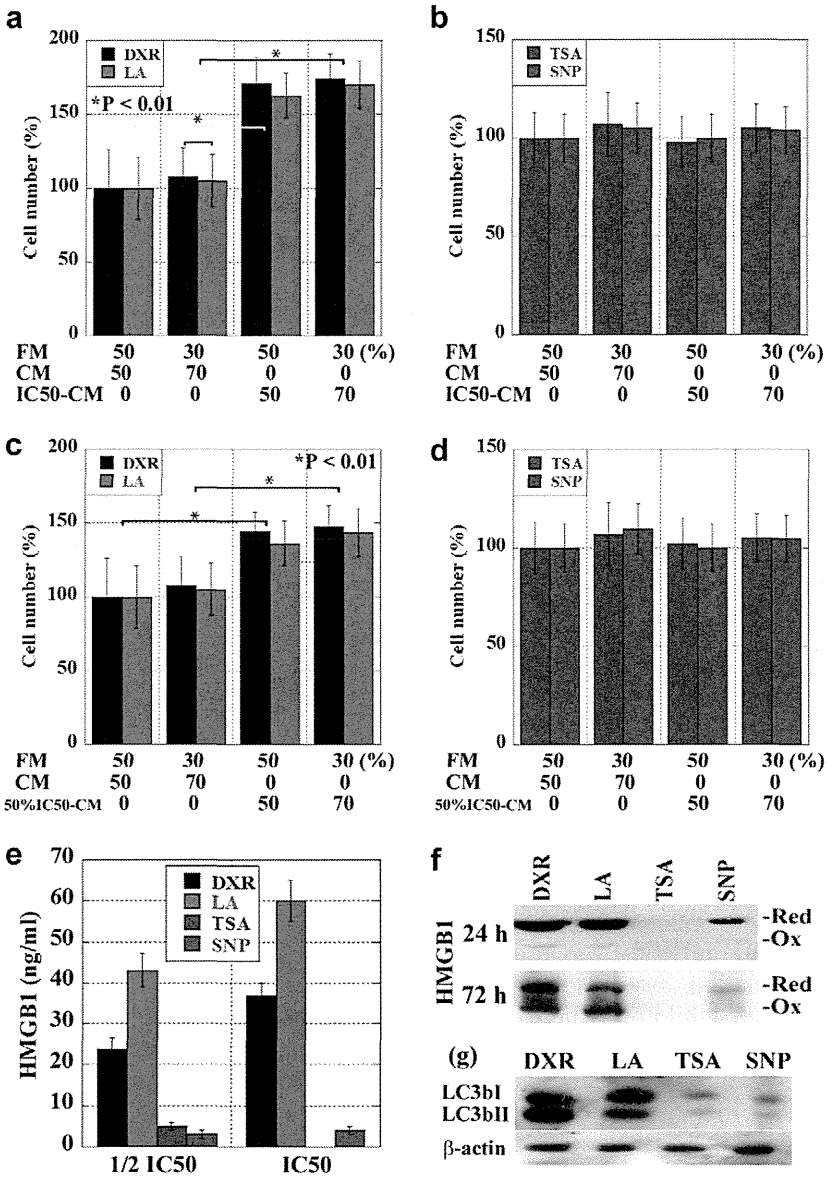

Fig. 2. Effect of culture medium (CM) from cell death inducer-treated CT26 cells on cell growth. (a–d) CT26 cells were incubated for 24 h with CM from CT26 cells treated with an 50% inhibitory concentration (IC50) of doxorubicin (DXR) or linoleic acid (LA) (a and c) and trichostatin A (TSA) or sodium nitroprusside (SNP) (b and d), mixed with fresh medium. FM, fresh medium; CM, culture medium of PBS-treated cells; IC50-CM, culture medium of cell death inducer-treated cells at the IC50 concentration. 50% IC50-CM, culture medium of cell death inducer-treated cells at 50% of the IC50 concentration. (e) HMGB1 concentration in the CM of CT26 cells treated with SNP, TSA, LA and DXR was determined by enzyme-linked immunosorbent assay (ELISA). (f) Oxidised HMGB1 was examined by sodium dodecyl sulphate–polyacrylamide gels (SDS–PAGE) in a non-reducing condition and immunoblotting. Red; reduced form, Ox, oxidised form. (g) Expression of autophagy-related microtubule-associated protein light chain (LC3) was examined by immunoblotting. Error bars represent standard deviation (SD).

tumour and the growth of contralateral tumours were monitored after injection of DXR or TSA (Fig. 4a–c). The serum concentration of HMGB1 was higher in the DXR-treated mice than in the TSA-treated mice (Fig. 4a). Regrowth of tumours injected with DXR was faster than that of the tumours injected with TSA (Fig. 4b). Moreover, growth of contralateral tumours was faster in the DXR-treated mice than in the TSA-treated mice (Fig. 4c). The difference of effects between DXR and TSA on tumour regrowth and the growth of contralateral tumours were confirmed by LL2 murine lung cancer cells in C57BL6 mice and HT29 human colon cancer cells in nude mice (Fig. 4d–f).

In the next set of experiments, anti-HMGB1 antibody was administered on days 8–10 in the same bilateral tumour model (Fig. 4g–i). The serum concentration of HMGB1 in DXR-treated mice was found to be reduced to the level observed in the TSA-treated mice (Fig. 4g). Furthermore, regrowth of tumours injected with DXR and growth of contralateral tumours in the DXR-treated mice was not statistically different from that observed in the TSA-treated mice (Fig. 4h–i).

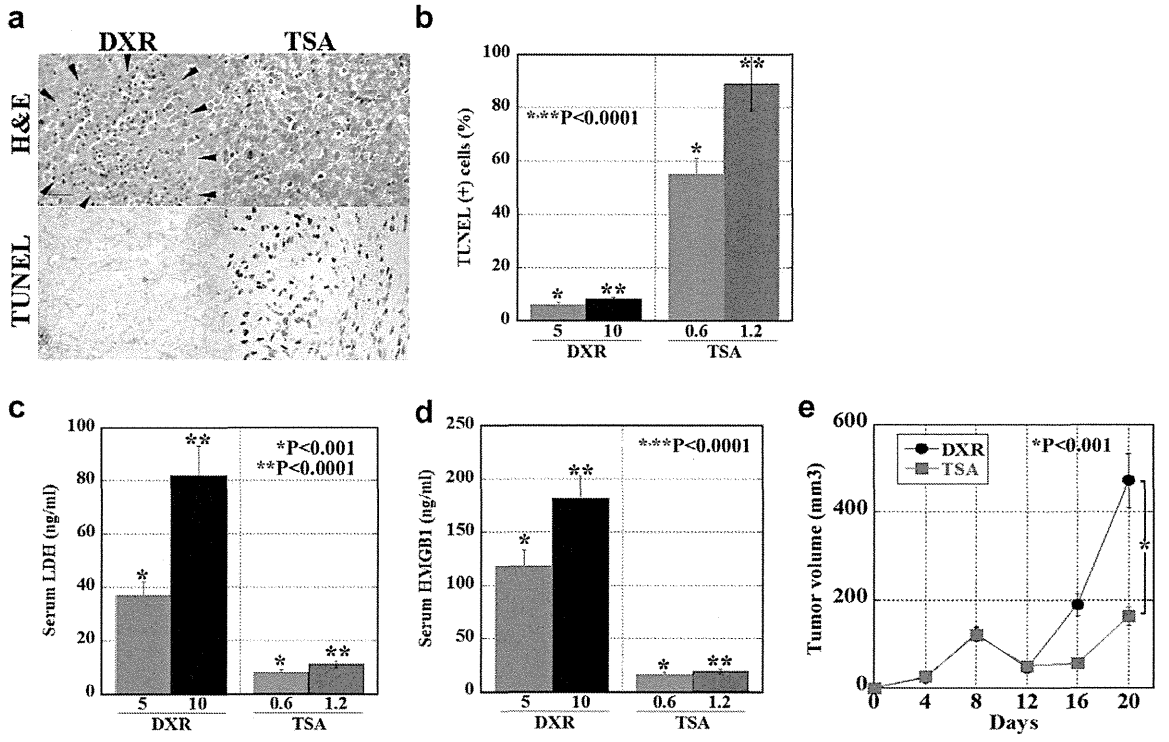

Fig. 3. Effect of cell death inducers on subcutaneous CT26 tumours. (a) Histological appearance of CT26 tumours treated by intraperitoneal (i.p.) injection of doxorubicin (DXR) or trichostatin A (TSA) at 50% inhibitory concentration (IC50) and 1/2 IC50 concentrations. H&E staining revealed necrotic changes (arrowheads). A Terminal deoxynucleotidyl transferase (TdT)-mediated dUTP-biotin nick end labelling (TUNEL) assay showed apoptotic cells with brown nuclei. Bar represents 50 μm. (b) The frequency of apoptotic cells was examined in 2000 cells. (c and d) Serum LDH and HMGB1 concentrations (ng/ml) were determined by enzyme-linked immunosorbent assay (ELISA). (e) The growth of subcutaneous tumours treated with DXR or TSA. Error bars represent standard deviation (SD).

The effect of anti-HMGB1 antibody was examined between post- and pre-inoculation dosage (Fig. 4j–l). In comparison with the tumour-inhibitory effect of the post-inoculation treatment with the antibody, no effect was found by the pre-inoculation treatment. The effect of EP was also examined (Fig. 4j–l). EP inhibited translocation and secretion of HMGB1.[27,29] EP treatment inhibited tumour growth by both post- and pre-inoculation administration; however, the latter showed more pronounced effect. The inhibitory effect of the antibody and EP was related with HMGB1 concentrations (Fig. 4l).

3.5. Effect of cell death on metastasis

We next examined the effect of cell death on metastasis by using mouse models of metastasis (Fig. 5). In the lung metastasis model, the lung weight and number of metastatic foci were more pronounced in the DXR-treated mice than in the TSA-treated mice (Fig. 5a and b). Similarly, in the liver metastasis model, the size and number of metastatic foci were also more pronounced in the DXR-treated mice (Fig. 5c and d). However, concurrent treatment of anti-HMGB1 antibody with administration of DXR abrogated the enhancement of metastasis to both the lung and liver.

To examine the effect of cell death inducers on tumour dormancy, we used the LA-induced dormancy model (Fig. 5e).[26] Inoculated quiescent CT26 cells regrew to form tumours in the DXR-treated mice; however, no tumours were formed in the TSA-treated mice. Concurrent treatment with anti-HMGB1 antibody and DXR administration abrogated the dormancy break.

To confirm the anti-HMGB1 antibody on the signal transduction, phosphorylation of ERK1/2 was examined (Fig. 5f). Concurrent treatment of anti-HMGB1 antibody with DXR reduced the phosphorylation of ERK1/2 to the same level to those of untreated or TSA-treated tumours.

Histopathology of the metastatic foci in the lung and liver of tumours treated with DXR, TSA and DXR + anti-HMGB1 antibody was not different from that in the control. Then expressions of MIB1 and MMP2 were examined in the metastatic foci (Fig. 5g). Both expressions were higher in DXR-treated groups than those in the groups treated with TSA, anti-HMGB1 antibody or the untreated control group.

3.6. Effects of HMGB1 on innate immunity and cancer cell survival

HMGB1 plays a role in both cancer cells and immune cells via the RAGE and TLR4 receptors. Thus, we examined the effects of the balance of RAGE and TLR4 on the function of HMGB1 in cancer cells and

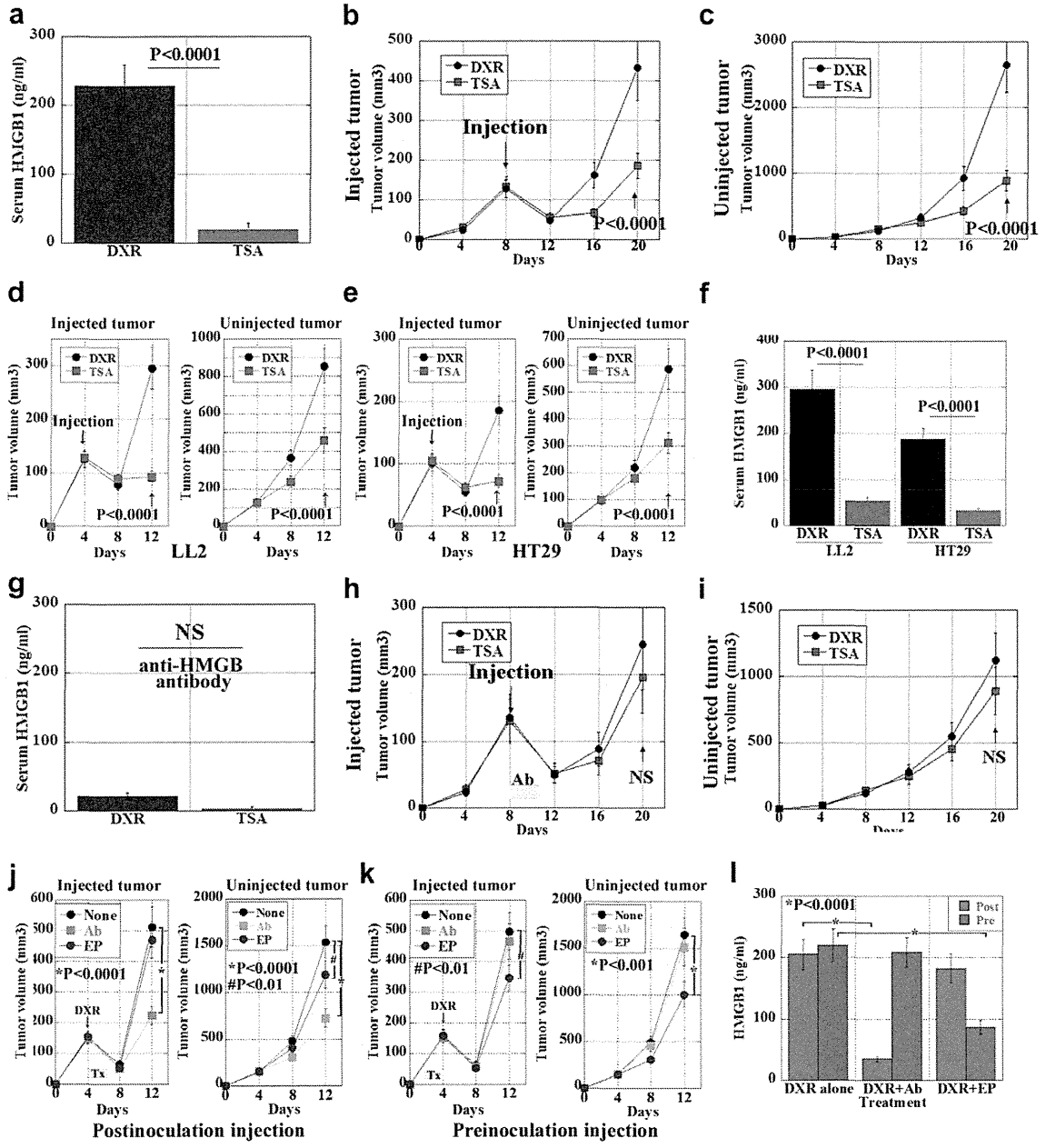

Fig. 4. Effect of cell death induction on regrowth of remnant cancer cells. (a–c) In a bilateral subcutaneous tumour model using CT26 cells in BALB/c mice (1×10^7 cells), doxorubicin (DXR) or trichostatin A (TSA) was injected into the tumour on 1 side of the mouse on day 8. (d–f) The bilateral tumour model using LL2 and HT29 cells in C57/BL6 mice and nude mice (1×10^8 cells). (g–i) In the same bilateral subcutaneous tumour model using CT26 cells in BALB/c mice (1×10^7 cells), anti-HMGB1 antibody (Ab) was administered intraperitoneally on days 8–10. (j–l) In the same bilateral subcutaneous tumour model using CT26 cells in BALB/c mice (1×10^8 cells), anti-HMGB1 antibody (Ab) or ethyl pyruvate (EP) was administered on days 4–6 (postinoculate) or on days 2–4 (preinoculate). (a, f, g, and l) Serum HMGB1 concentration was determined by enzyme-linked immunosorbent assay (ELISA) on day 9. (b, d-left, e-left, h, j-left, k-left) Regrowth of the injected tumours. (c, d-right, e-right, I, j-right, k-right) The growth of contralateral tumours. Error bars represent standard deviation (SD).

macrophages (Fig. 6). U937 monocytic cells were treated with CM from CT26 cells treated with DXR (DXR-CM) or TSA (TSA-CM) (Fig. 6a). DXR-CM treatment induced tumour necrosis factor-α (TNF-α) secretion from U937 cells, with a peak of neutralisation at 20 ng/ml of anti-HMGB1 antibody. In contrast, TSA-CM did not affect TNF-α secretion from U937 cells. U937 cells treated with HMGB1 showed induction of TNF-α secretion, with a peak at 20 μg/ml of HMGB1; however, U937 cell numbers were decreased in an HMGB1 dose-dependent manner (Fig. 6b). U937 cells expressed both RAGE and TLR4 (Fig. 6c). U937 cells with TLR4 knockdown failed to secrete TNF-α, whereas U937 cells with RAGE knockdown did not show inhibition of HMGB1-induced TNF-α secretion (Fig. 6d and e).